RSC Advances

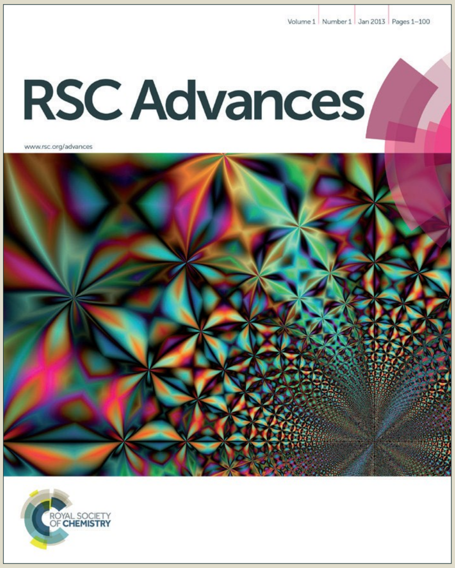

ROYAL SOCIETY OF CHEMISTRY

www.rsc.org/advances

RSC Advances

ARTICLE

Silica-coated gradient alloy quantum dots with high luminescence for converter materials in white light-emitting diodes

Received 00th January 20xx,
Accepted 00th January 20xx

DOI: 10.1039/x0xx00000x

www.rsc.org/

Hak-Sung Jung,[‡,a,e] Young-Jae Kim,[‡,a, b] Junsang Cho,[a, c] Tae-Jong Yoon,*[d] and Jin-Kyu Lee*[a]

Hydrophobic gradient alloy quantum dots (QDs) were prepared through a facile organic route. The amphiphilic, non-ionic polymer (PVP) was absorbed onto the surface of QDs, and therefore, the PVP coated QD (QD@PVP) could be dispersible in both polar and non-polar solvents. The QD@PVP was dispersed in ethanol and added tetraethyl orthosilicate (TEOS) with a basic catalyst in order to generate silica shell encapsulated QD (QD@SiO_2). We report a preparation method for QD@SiO_2 that maintains their high luminescence and thermal- and photo-stability using dimethylamine (DMA) as a basic catalyst. A white light-emitting-diodes (WLEDs) incorporating the QD@SiO_2 exhibited good performance in terms of superior luminescence efficiency and high color purity.

Introduction

The synthesis of nanometer-scale materials is a very important research field of nanotechnology. In particular, semiconductor quantum dots (QDs) have attracted much interest from academia and industry because they have many potential applications, such as in biosensors, light-emitting devices, photovoltaic devices, and memory devices.[1-4] QDs are considered to be among the most promising light emitters for next-generation displays and solid-state lighting because of their superior optical properties, such as their broad absorption, narrow emission bandwidth, easy control of the emission wavelength, and superior solid-state luminescence efficiency compared with conjugated molecules (polymers) or inorganic phosphors.[5, 6] After the first demonstration of QD-based light-emitting diodes (QLEDs), the performance of QLED devices has rapidly improved because of technological developments and the accumulation of fundamental knowledge.[7] Based on the wide range of studies performed on QLEDs, such as understanding the exciton-decay dynamics, designing device structures from different concepts, and synthesizing the composition and structure of the QDs, highly efficient and bright QLEDs have been successfully produced with easily reproducible methods.[8-10]

However, the advances achieved in QLED performance have mostly been limited to white light-emitting QLEDs, and there are still problems with retaining the initial optical properties of the QDs during device fabrication and with their long-term stability.[11] In general, the optical properties of QDs are extremely sensitive to their surface chemistry and chemical environment. The coordinating organic ligands used to passivate the surface of QDs during their growth remain on the surface after their preparation and are strong contributors to bulk QD optical properties, including emission quantum yields (QYs). Unfortunately, the high QYs of QDs are considerably reduced after the repeated cycles of QD purification or the integration processing required for creating solid-state QD films. This is because the optical properties of the quantum dots are significantly affected by basic catalysts, polar solvents and ligand exchange processes.[12, 13]

To overcome the aforementioned problems, the idea of encapsulating QDs in silica shells has been extensively explored because the silica shells can enhance the stability of QDs.[14-16] The methods for incorporating QDs into silica shells are roughly divided into techniques based on either a Stöber method or reverse micelle synthesis. Reverse micelle synthesis uses a reversed micro-emulsion system (water-in-oil (W/O)), where small water droplets are stabilized by a nonionic surfactant in a continuous hydrophobic phase.[17, 18] This synthetic strategy can easily yield more uniformly sized silica particles because the size of the water pool, which is the reaction field for the formation of silica particles, is rather uniform. However, this method is limited by low yields and the

---

[a] *Dr. H.-S. Jung, Dr. Y.-J. Kim, J. Cho and Prof. J.-K. Lee*
Department of Chemistry, Seoul National University, Seoul 151-747, Korea.
E-mail: jinklee@snu.ac.kr
[b] *Dr. Y.-J. Kim*
Current Address: Program in Nano Science and Technology, Graduate School of Convergence Science and Technology, Seoul National University, Seoul 151-742, Korea.
[c] *J. Cho*
Current Address: Department of Chemistry, Texas A&M University, College Station, Texas, USA, 77843.
[d] *Prof. T.-J. Yoon*
College of Pharmacy, Ajou University, 206, World cup-ro, Yeongtong-gu, Suwon-si, Gyeonggi-do, 16499, South Korea
E-mail: tjyoon@ajou.ac.kr
[e] *Current address (Dr. H.-S. Jung)*
Lab. Of Molecular Biophysics, National Heart, Lung and Blood Institute, NIH, 50 South Drive, Build 50, Bethesda, Maryland 20892, USA

† Electronic Supplementary Information (ESI) available: PL spectra of QDs, QDs@PVP, and QD@SiO_2-based WLED, DLS data and TEM images of QDs@SiO_2. See DOI: 10.1039/x0xx00000x

‡ These authors contributed equally to this work.

use of surfactants necessitates extensive washing to remove the surfactant molecules, which might interfere with the properties of the QDs, before being used for any application.[19]

The alternative is the Stöber process, which involves the addition of tetraethyl orthosilicate (TEOS) to stable "seed" particles in an ethanol solution that contains water and ammonia as a catalyst to create monodisperse, spherical, electrostatically stabilized particles.[20] Therefore, the surface of the QDs must be treated with more polar ligands to enable their transfer into ethanol. However, the optical properties of QDs still decreased during silica shell coating process, and an improved preparation method should be developed.[21]

Experimental

Materials

All air- and/or moisture-sensitive compounds were handled with standard Schlenk line techniques or in a glove-box under a nitrogen atmosphere. $Zn(OAc)_2{\cdot}2H_2O$, 1-octadecene (ODE), oleic acid (OA), oleylamine (OLAm), sulfur shot, polyvinylpyrrolidone (PVP), and a dimethylamine solution (DMA; 40%) were purchased from Aldrich. Tri-n-octylphosphine (TOP; 85%) and tetraethyl orthosilicate (TEOS) were purchased from TCI. CdO was purchased from Alfa Aesar. Selenium shot was purchased from Acros. Ethanol (EtOH) was purchased from J. T. Baker. Chloroform was purchased from Samchun Chemical Co. All organic solvents were used without any further purification. Surface mount device (SMD) 5050 blue LED chips were purchased from ENTEC L&E Ltd. An optical encapsulant kit (OE-6560 A/B kit) was purchased from Dow Corning Korea Ltd.

Preparing the mixed chalcogenide stock solutions

Both the selenium shot (0.03158 g, 0.4 mmol) and sulfur shot (0.1282 g, 4.0 mmol) were weighed into a vial in the glove-box. 3 mL of TOP (2.49 g, 6.72 mmol) was added to the vial and the mixture was stirred overnight until all the solids were dissolved and the solution became clear and colorless for the synthesis of the green-emitting gradient alloy QDs. This solution was stored at room temperature in the glove-box until being used.

Synthesis of Green-Emitting Gradient Alloy QDs (GQD)

The gradient alloy QDs were synthesized according to a procedure similar to that previously in the literature.[22] For the synthesis of the GQDs (λ_{em} = 535 nm), CdO (0.051 g, 0.4 mmol) and $Zn(OAc)_2{\cdot}2H_2O$ (1.098 g, 5.0 mmol)) were weighed into a 100 mL two neck round bottom flask equipped with a condenser and thermocouple adapter. After OA (6.105 g, 21.6 mmol) and ODE (7.89 g, 10 mL) were added to the flask, the mixture was heated to 180 °C until all the solids in the flask were dissolved , *i.e.*, a clear solution, to generate the metal precursors Cd–OA and Zn–OA. The solution was degassed at 150 °C under vacuum for 20 min to remove the water produced by the reactions. The mixture was then heated to 300 °C and the mixed chalcogenide stock solution containing Se (0.03158 g, 0.4 mmol) and S (0.1284 g, 4.0 mmol) dissolved in 3 mL of TOP was swiftly injected into the reaction flask. The temperature was reduced to 280 °C for the following growth step.

Synthesis of Red-Emitting Gradient Alloy QDs (RQD)

For the synthesis of the RQDs (λ_{em} = 615 nm), CdO (0.1284 g, 1.0 mmol) and $Zn(OAc)_2{\cdot}2H_2O$ (0.878 g, 4.0 mmol) were placed in a 100 mL two neck round bottom flask. After OA (5.643 g, 20.0 mmol) and ODE (7.89 g, 10 mL) were added to the flask, the mixture was heated to 180 °C until all the solids in the flask were dissolved to generate the metal precursors Cd–OA and Zn–OA. The solution was degassed at 150 °C under vacuum for 20 min to remove the water produced by the reactions. After the mixture was heated to 300 °C, 0.4 mL of a 1 M TOP solution containing Se (0.03158 g, 0.4 mmol) was injected first into the mixture solution, and 30 s later, 4 mL of a 1 M TOP solution containing S (0.1284 g, 4.0 mmol) was injected into the reaction flask. The temperature was set to 280 °C for the following growth step.

Preparation of QD@PVP

PVP (100 mg, which corresponds to 1300 kg mol^{-1}) was dissolved in the QD solution (1 mL, 10 mg of QDs per mL of chloroform; the actual weight of the QDs was measured after vacuum drying an appropriate portion of the purified QD solution). By directly adding the mixed solution of QDs and PVP into ethanol, the PVP-stabilized nanoaggregates (QD@PVP) were formed and used in the next step without removing the small amount of $CHCl_3$.

Synthesis of QD@SiO_2

TEOS (0.1 mL) was added to a well-stirred dispersion of the QD@PVP in ethanol (5.0 mL, 1 mg of QDs per mL of ethanol), the preparation of which is described above, and the mixture was stirred for 10 min at room temperature. The DMA solution (0.1 mL, 40 wt% in water) and 0.1 mL of distilled water were then added to the mixed solution. After 12 h of stirring, the QD@SiO_2 was isolated by centrifugation at a speed of 20,000 rpm for 20 min and the supernatant was removed. The isolated QD@SiO_2 was then re-dispersed in ethanol. This washing process of centrifugation followed by re-dispersing the QD@SiO_2 in ethanol was repeated 3 times. Finally, the re-dispersed QD@SiO_2 solution was centrifuged at a speed of 4,000 rpm to remove any aggregated particles and the supernatant was obtained.

Fabrication of QD@SiO_2-assisted phosphor-converted WLEDs

WLEDs were fabricated by combining the InGaN-based blue LEDs with the as-synthesized red- and green-emitting QD@SiO_2 and OE-6560 resin. The QD@SiO_2 was dispersed in acetone to avoid aggregation after being mixed with the OE-6560B resin. The mixed solution was blended with a vortex mixer for 15 min until the mixture became transparent. Next, the acetone was removed *in vacuo*. The QD@SiO_2/OE-6560B resin mixture was further mixed with the OE-6560A resin at a weight ratio of 1:3 (OE-6560A:OE-6560B). The mixture was stirred until it became homogeneous. The mixture was then dropped onto the blue LED and heated in an oven at 80 °C for 30 min and finally at 170 °C for 90 min.

Preparation of the free-standing film

A QD@SiO$_2$/silicone polymer nanocomposite film was prepared by spin-coating slide glass with the QD/silicone polymer solution at 2000 rpm for 120 sec and then curing the film at 170 °C for 30 min. The free-standing film was obtained by peeling it off the slide glass.

Photostability test

The GQD@SiO$_2$ and RQD@SiO$_2$ were dispersed in water. Samples were then exposed to the light of a tungsten halogen lamp (200 W, PHILIPS) with a light intensity of 757 mW/cm^2. The emission spectra of all of the samples were measured after appropriate illumination times.

Characterizations. The absorption and emission spectra of the QDs and QD@SiO$_2$ were measured at room temperature with UV-Vis spectrometry (Sinco, S-3100) and fluorophotometry (JASCO, FP-6500), respectively. The absolute quantum yield of QD solutions was obtained by absolute PL quantum yield (QY) measurement system QE-1200 (OTSUKA Electronics) excited at 430 nm. The size and shape of the QDs and QD@SiO$_2$ were characterized with transmission electron microscopy (TEM, JEOL, JEM-2100). Hydrodynamic size of QD@SiO$_2$ in ethanol was measured three times and averaged at room temperature using the dynamic light scattering (DLS, Zetasizer Nano ZS, Malvern instruments). The electroluminescence spectra, CIE and chromaticity coordinates of the as-fabricated QD@SiO$_2$-based LED were measured at room temperature with a quantum efficiency measurement system (QE-1200, OTSUKA Electronics).

Results and discussion

We successfully incorporated QDs emitting green or red light into silica shells while retaining their initial photoluminescence (PL) efficiency by using polyvinylpyrrolidone (PVP) and DMA as the basic catalyst (Scheme 1). The QDs were prepared according to a previously reported method using four precursors (Cd–OA, Zn–OA, Se-containing TOP, and S-containing TOP) that are reacted to grow the gradient alloy shell ($CdSe_{y1}S_{1-y1}/ZnSe_{Y2}S_{1-y2}$).[22] The structural and optical properties of the as-synthesized QDs were characterized by TEM, UV-Vis and PL spectroscopy (Fig. 1).

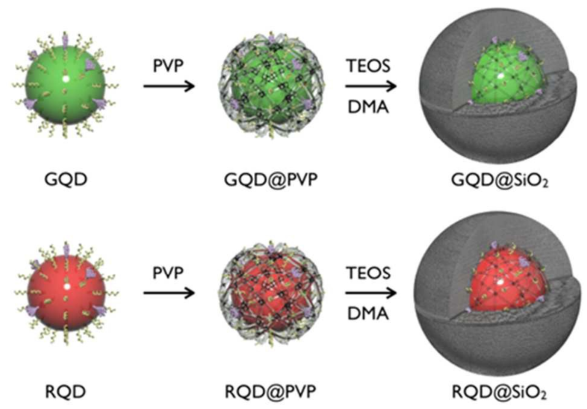

Scheme 1 Synthesis of silica shell coated quantum dot (QD) nanoparticles. The prepared GQD and RQD were soluble only in a non-polar organic solvent such as chloroform, but the PVP-fabricated QDs were dispersible in relative polar organic solvents such as ethanol. Eventually, the silica shell-coated QDs (GQD@SiO$_2$ or RQD@SiO$_2$) were simply prepared by a base catalyst (DMA).

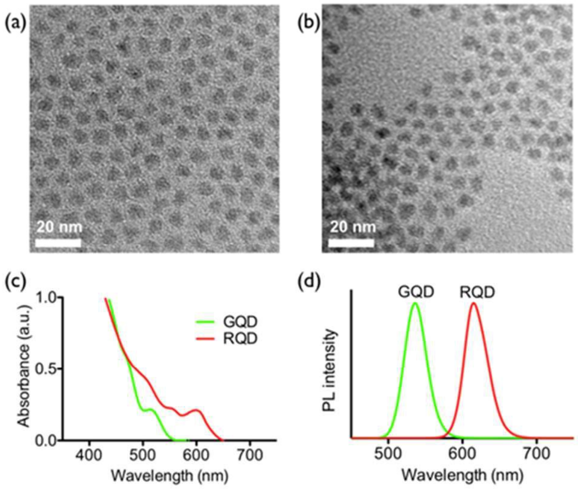

Fig. 1 TEM images of GQD (a) and RQD (b) with regular size distributions. UV-Vis absorption (c) and PL (d) spectra of the synthesized QDs in chloroform. The shoulder peaks of absorption are at 512 (GQD) and 600 (RQD) nm. The PL intensities were normalized to the values at 540 (GQD) and 620 (RQD) nm

From the data, the QDs were determined to be ~ 7 nm in diameter with a regular distribution. The embedding of these hydrophobic QDs in silica particles *via* the Stöber method occurs in an alcoholic solution. PVP is amphiphilic because it has a highly polar amide group within the pyrrolidone ring and apolar methylene and methine groups in the ring and along its backbone.[23, 24] For this reason, PVP-coated QDs can be easily and uniformly dispersed in ethanol without any aggregated precipitates forming in the alcoholic solution. Therefore, the silica shells are successfully grown by the consecutive addition of TEOS with a basic catalyst.

We optimized the silica shell coating of the QDs to maintain the high PL efficiency and good stability by controlling the reaction conditions. The PL intensities of the as-prepared QD and PVP-modified QD (QD@PVP) dispersed in chloroform did not exhibit significant changes (Fig. S1†). The formation of the SiO$_2$ shells involves the base-catalyzed hydrolysis of TEOS and the subsequent condensation onto the QD surface. In most cases, ammonia (NH_4OH) would be added as a catalyst to accelerate the deposition process.[25-27] However, it has been reported that the silica shells grown on the surface of QDs, as well as water and ammonia, can affect the optical properties.[28, 29] Therefore, the basic catalyst plays a major role in the potential degradation of the original luminescence of the QDs during the formation of the silica shells through sol-gel condensation.

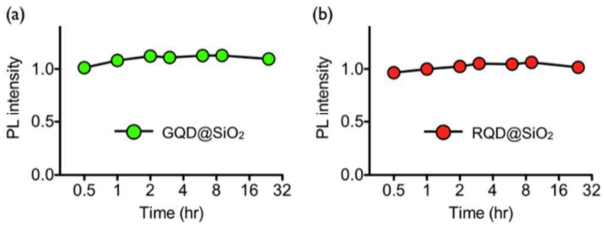

Fig. 2 Monitoring of PL intensity for QD@SiO_2 nanoparticle in ethanol solution as times. There was no significant change of intensity. The intensities were normalized at 540 nm (GQD@SiO_2) and 620 nm (RQD@SiO_2).

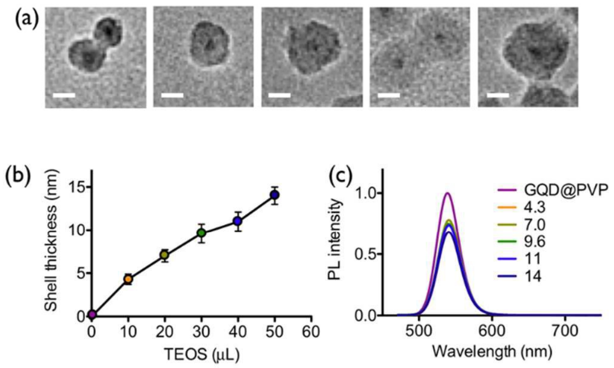

Fig. 3 TEM images of GQD@SiO_2 particles with different silica shell thicknesses (a). Each scale bar is 10 nm. The shell thickness could be controlled by adjusting the TEOS concentration (b) and was measured from the low magnification TEM images (Fig. S6). The PL intensity of GQD based particles gradually decreased as the silica shell thickness increased (c).

To study the effect of the base catalyst on the PL properties of QDs, the PL intensity of QD@PVPs dispersed in ethanol with the same concentration of NH_4OH or DMA was monitored over time (Fig. S2†). In the case of NH_4OH, the PL intensity of the GQD@PVP gradually decreased to approximately 50 % of the initial intensity after 24 hr. Furthermore, the RQD@PVP in the mixed NH_4OH and ethanol solution did not have a high solubility and precipitated within 3 hr (Fig. S3†). On the contrary, the use of DMA did not cause significant changes in either the intensity of the PL spectra or solubility. We realized that the NH_4OH base catalyst could damage the QD@PVP particle surface. We thought that a secondary (2’) - amine catalyst such as DMA did not directly attach to the surface of the QD nanoparticles because of steric hindrance but that a 1’- amine such as NH_4OH easily contacted and passivated the particle surface.[30-32]

To investigate the effects of the reaction conditions on the PL properties of the QDs after being coating with SiO_2 shells, the PL spectra and maximum PL intensity of the gradient alloy QDs@SiO_2 were measured for 24 h (Fig. 2). Under the same reaction conditions, the initial maximum PL intensities of the GQDs@SiO_2 and RQDs@SiO_2 are maintained. With the SiO_2 shells, the PL spectra of the QDs do not exhibit any significant changes. Initial PL quantum yield was maintained in case of GQD, however, that of RQD is gradually decreased after PVP and silica coating (Table 1S†). Even though small decrease in QY are found, the reaction conditions of the encapsulation process are suitable for maintaining the optical properties of QDs.

Table 1 Comparison data for the various QD based particle solution. The PL efficiency of the GQD@SiO_2 was calculated by determining the integrated PL emission spectrum of all samples with 450-nm-wavelength excitation.

Sample	TEOS (μL)	Silica shell thickness (nm)[a]	FWHM (nm)	λ_{max} PL (nm)	PL efficiency (%)[b]
GQD@PVP	N/A	N/A	35	539	100
1	10	4.3±0.6	36	541	77
2	20	7.0±0.7	36	541	80
3	30	9.6±1.1	36	541	76
4	40	11±1.1	36	541	75
5	50	14±1.0	36	540	69

[a] The mean size was determined from the TEM images. [b] PL efficiency was calculated from the PL emission spectra.

We optimized the preparation conditions used to coat the silica shells onto the QDs by controlling both the reaction time and TEOS concentration (Fig. S4, S5 and S7†). The silica shell formed very quickly, and the thickness saturated after 12 hr. This result is in good agreement with the observation of the hydrodynamic size of QD@SiO_2 confirmed by DLS. In addition, QDs were individually coated with silica shell without any aggregation during the encapsulating procedure (Fig. S6† and Table S2). In contrast, the thickness of the silica shell was proportional to the TEOS concentration (Fig. 3). These results indicate that the shell thickness can be precisely controlled by changing the concentration of TEOS added. In addition, we examined the effects of the silica shell thickness on the optical properties of the GQD@SiO_2 in ethanol (Table 1). The PL efficiencies of all the GQDs@SiO_2 samples were revealed ~ 70 % of that of the GQD@PVP and the maximum PL intensity wavelength and FWHM of the GQDs was retained. This means that the silica-coated QDs maintain their spectral purity, which can be attributed to the isolation of the QDs in the silica shells. These results correspond well with the TEM images. In addition, all samples were re-dispersed in ethanol without any aggregation or significant changes to the PL properties. This means that the encapsulating process of the Stöber method is

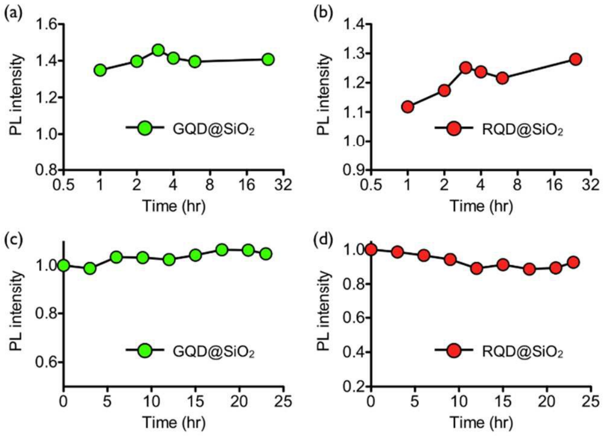

Fig. 4 Photo- thermal-stability of the QD@SiO_2 in solution. The PL intensity was measured after various times of exposure to a tungsten halogen light (a and b) and the PL intensity was also monitored as a function of aging time at 120 °C (c and d).

effective for producing homogeneously sized and highly luminescent QDs@SiO_2.

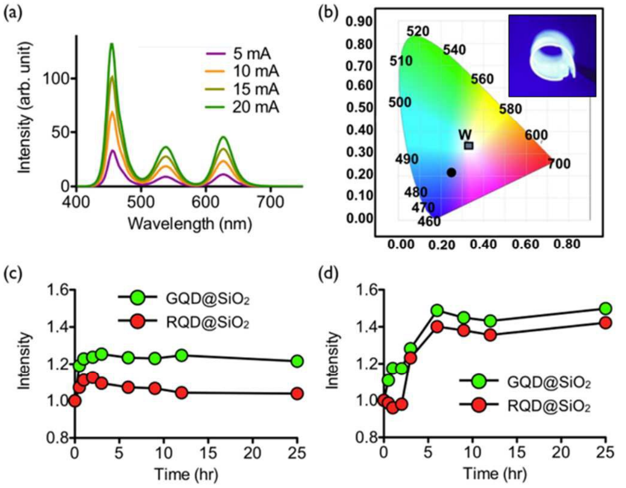

Fig. 5 Spectra of the QD@SiO_2 based WLED at different operating currents (a). Commision Internationale de l'Eclairage (CIE) chromaticity coordinates of the QD@SiO_2-based WLED (b). The inset shows the QD@SiO_2/silicon polymer nanocomposite film when illuminated with the InGaN-based blue LED (60 mA). Changes in the emission intensities of the QD@SiO_2/silicon polymer film under the blue LED at powers of 0.5 (c) and 1 W (d). The PL intensities of the GQD@SiO_2 and RQD@SiO_2 were normalized at 540 and 620 nm, respectively.

The optical properties of the prepared QD@SiO_2 were determined under various conditions to assess the photo-stability and thermal stability, as shown in Fig. 4. From the results, the QD@SiO_2 in the aqueous solution did not exhibit photo-bleaching over time by exposure to the tungsten halogen lamp. After being exposed to continuous irradiation, an initial enhancement of the PL intensity of the GQDs@SiO_2 can be seen, and the PL intensity remains close to the elevated value. On the other hand, the PL intensity of the RQDs@SiO_2 gradually increases over time (called "photobrightening"). Although the mechanisms explaining this type of photobrightening are still not clearly understood, there have been several groups reporting the mechanisms of analogous systems, including the passivation of surface states, suppression of the ionization rate, photochemical annealing, and desorption of surfactants.[33-35]

Because the temperature of light-emitting diodes (LEDs) devices can reach 120 °C,[36] we investigated the thermal stability of the QD@SiO_2 particles at that temperature. The powder-formed QD@SiO_2 particles were treated for various aging times at 120 °C, and the PL intensity was determined after dispersing the particles in solution. The prepared QD@SiO_2 using the DMA catalyst exhibited superior optical performance in the stability investigation.

For application as the light conversion material for blue InGaN-based LEDs, the QD@SiO_2 were dispersed in acetone and mixed with a silicone polymer.[37] (7.5 wt% nanoparticles, RQD@SiO_2:GQD@SiO_2 = 1:5, w/w). In our system, we thought that the changes the intensity (increasing red and decreasing green intensity) after formation of composite was in accordance with the re-adsorption mechanism. The electroluminescence (EL) spectra of the as-fabricated QD@SiO_2-based white LED (WLED) under different forward bias currents are shown in Fig. 5a. The emission peaks of the blue LED chip, GQD@SiO_2 and RQD@SiO_2 are located at 460 nm, 540 nm and 620 nm, respectively. The inset image in Fig. 5b indicates superior performance with high luminescence from the flexible polymer film. As shown in Fig. 5b, the Commission Internationale de l'Eclairage (CIE) color coordinates of the QD@SiO_2-based WLED are (0.24, 0.21), which corresponds to a cool white light that is commonly used for display back-lights.[38]

To verify the stability of the QD@SiO_2/silicone polymer composite, we measured the maximum PL intensity (Fig. 5c, d and Fig. S8†) at various times. The PL intensity of the QD-based polymer composite increased slightly during the first 3 hr and then remained approximately constant until 24 hr for the 0.5 W LED operating power. Interestingly, when the LED was operated at 1 W, the composite intensity increased dramatically to approximately 150 % at 5 hr. We thought that the photo-enhancement effect was attributed to an increase in the PL of the composite.[39] We suggest that the QD@SiO_2/polymer nanocomposite films are very flexible with high luminescence and are potentially suited to various device applications.

Conclusions

We successfully incorporated QDs emitting at green and red wavelengths into silica shells while retaining their initial optical properties using the dimethylamine basic catalyst. This simple method places a single QD within each silica nanoparticle, which maintains the spectral purity. The QD@SiO_2 retained their initial PL intensity under photo- and thermal stress. Therefore, the QD@SiO_2 was utilized a green and red color converters with a blue LED to prepare the WLED for a display backlights and exhibited excellent WLED performance because of their high stability. We suggest that our QD@SiO_2 particle system have great potential as color-converting materials in the next generation of LEDs.

Acknowledgements

Authors thank J.-H. Kim and B.-H. Sohn for the PL measurements of the QD@SiO_2-based WLED. Y.-J. Kim was supported by the BK21 plus program and H. –S. Jung was supported by a grant of the Korea Health Technology R&D project through the Korea Health Industry Development Institute (KHIDI), funded by the Ministry of Health & Welfare, Republic of Korea (HI15C0979). T.-J. Yoon was supported by a grant from the Osong Medical Innovation Foundation R&D project (HO13C0009) of the Ministry of Health and Welfare in South Korea.

References

1. U. Resch-Genger, M. Grabolle, S. Cavaliere-Jaricot, R. Nitschke and T. Nann, *Nat. Methods*, 2008, **5**, 763-775.
2. A. J. Shields, *Nat. Photonics*, 2007, **1**, 215-223.
3. J. B. Sambur, T. Novet and B. A. Parkinson, *Science*, 2010, **330**, 63-66.
4. M. Kroutvar, Y. Ducommun, D. Heiss, M. Bichler, D. Schuh, G. Abstreiter and J. J. Finley, *Nature*, 2004, **432**, 81-84.
5. J. Lim, S. Jun, E. Jang, H. Baik, H. Kim and J. Cho, *Adv. Mater.*, 2007, **19**, 1927-1932.
6. Q. Sun, Y. A. Wang, L. S. Li, D. Wang, T. Zhu, J. Xu, C. Yang and Y. Li, *Nat. Photonics*, 2007, **1**, 717-722.
7. V. L. Colvin, M. C. Schlamp and A. P. Alivisatos, *Nature*, 1994, **370**, 354-357.
8. H. Huang, A. Dorn, G. P. Nair, V. Bulović and M. G. Bawendi, *Nano Lett.*, 2007, **7**, 3781-3786.
9. J. M. Caruge, J. E. Halpert, V. Wood, V. Bulovic and M. G. Bawendi, *Nat. Photonics*, 2008, **2**, 247-250.
10. K.-S. Cho, E. K. Lee, W.-J. Joo, E. Jang, T.-H. Kim, S. J. Lee, S.-J. Kwon, J. Y. Han, B.-K. Kim, B. L. Choi and J. M. Kim, *Nat. Photonics*, 2009, **3**, 341-345.
11. S. Jun, J. Lee and E. Jang, *Acs Nano*, 2013, **7**, 1472-1477.
12. K.-H. Lee, J.-H. Lee, W.-S. Song, H. Ko, C. Lee, J.-H. Lee and H. Yang, *ACS Nano*, 2013, **7**, 7295-7302.
13. H. Chen, J. Ding, W. Guo, G. Chen and S. Ma, *RSC Advances*, 2013, **3**, 12327-12333.
14. D. Gerion, F. Pinaud, S. C. Williams, W. J. Parak, D. Zanchet, S. Weiss and A. P. Alivisatos, *J. Phys. Chem. B*, 2001, **105**, 8861-8871.
15. T. Nann and P. Mulvaney, *Angew. Chem. Int. Ed.*, 2004, **43**, 5393-5396.
16. M. Darbandi, R. Thomann and T. Nann, *Chem. Mater.*, 2005, **17**, 5720-5725.
17. R. Kumar, H. Ding, R. Hu, K.-T. Yong, I. Roy, E. J. Bergey and P. N. Prasad, *Chem. Mater.*, 2010, **22**, 2261-2267.
18. I. C. Serrano, Q. Ma and E. Palomares, *J. Mater. Chem.*, 2011, **21**, 17673-17679.
19. J. Cha, P. Cui and J.-K. Lee, *J. Mater. Chem.*, 2010, **20**, 5533-5537.
20. W. Stöber, A. Fink and E. Bohn, *J. Colloid Interface Sci.*, 1968, **26**, 62-69.
21. R. Koole, M. M. van Schooneveld, J. Hilhorst, C. de Mello Donegá, D. C. ’. Hart, A. van Blaaderen, D. Vanmaekelbergh and A. Meijerink, *Chem. Mater.*, 2008, **20**, 2503-2512.
22. J. Cho, Y. K. Jung and J.-K. Lee, *J. Mater. Chem.*, 2012, **22**, 10827-10833.
23. J. N. Smith, J. Meadows and P. A. Williams, *Langmuir*, 1996, **12**, 3773-3778.
24. C. Graf, D. L. J. Vossen, A. Imhof and A. van Blaaderen, *Langmuir*, 2003, **19**, 6693-6700.
25. B. Ji, E. Giovanelli, B. Habert, P. Spinicelli, M. Nasilowski, X. Xu, N. Lequeux, J.-P. Hugonin, F. Marquier, J.-J. Greffet and B. Dubertret, *Nat. Nanotechnol.*, 2015, **10**, 170-175.
26. D.-Y. Li, Y.-Z. Wang, X.-L. Zhao, X.-W. He, W.-Y. Li and Y.-K. Zhang, *J. Mater. Chem. B*, 2014, **2**, 5659-5665.
27. X. Wei, M. Meng, Z. Song, L. Gao, H. Li, J. Dai, Z. Zhou, C. Li, J. Pan, P. Yu and Y. Yan, *J. Lumin.*, 2014, **153**, 326-332.
28. C. Graf, S. Dembski, A. Hofmann and E. Rühl, *Langmuir*, 2006, **22**, 5604-5610.
29. S. Dembski, C. Graf, T. Krüger, U. Gbureck, A. Ewald, A. Bock and E. Rühl, *Small*, 2008, **4**, 1516-1526.
30. Y. Kobayashi, K. Misawa, M. Takeda, M. Kobayashi, M. Satake, Y. Kawazoe, N. Ohuchi, A. Kasuya and M. Konno, *Colloids and Surfaces A: Physicochemical and Engineering Aspects*, 2004, **251**, 197-201.
31. D. Nagao, E. Mine, Y. Kobayashi and M. Konno, *J. Chem. Eng. Jpn.*, 2004, **37**, 905-907.
32. Y. Kobayashi, H. Katakami, E. Mine, D. Nagao, M. Konno and L. M. Liz-Marzan, *J. Colloid Interface Sci.*, 2005, **283**, 392-396.
33. U. Takafumi, K. Junichi and Y. Yukio, *Nanotechnology*, 2004, **15**, 822-827.
34. M. A. Osborne and S. F. Lee, *ACS Nano*, 2011, **5**, 8295-8304.
35. D. B. Tice, M. T. Frederick, R. P. H. Chang and E. A. Weiss, *J. Phys. Chem. C*, 2011, **115**, 3654-3662.
36. S. Chhajed, Y. Xi, Y.-L. Li, T. Gessmann and E. F. Schubert, *J. Appl. Phys.*, 2005, **97**, 054506.
37. H.-S. Jung, Y.-J. Kim, S.-W. Ha and J.-K. Lee, *J. Mater. Chem. C*, 2013, **1**, 5879-5884.
38. E. Jang, S. Jun, H. Jang, J. Lim, B. Kim and Y. Kim, *Adv. Mater.*, 2010, **22**, 3076-3080.
39. Y. Ma, Y. Li, S. Ma and X. Zhong, *J. Mater. Chem. B*, 2014, **2**, 5043-5051.

Graphical Abstract

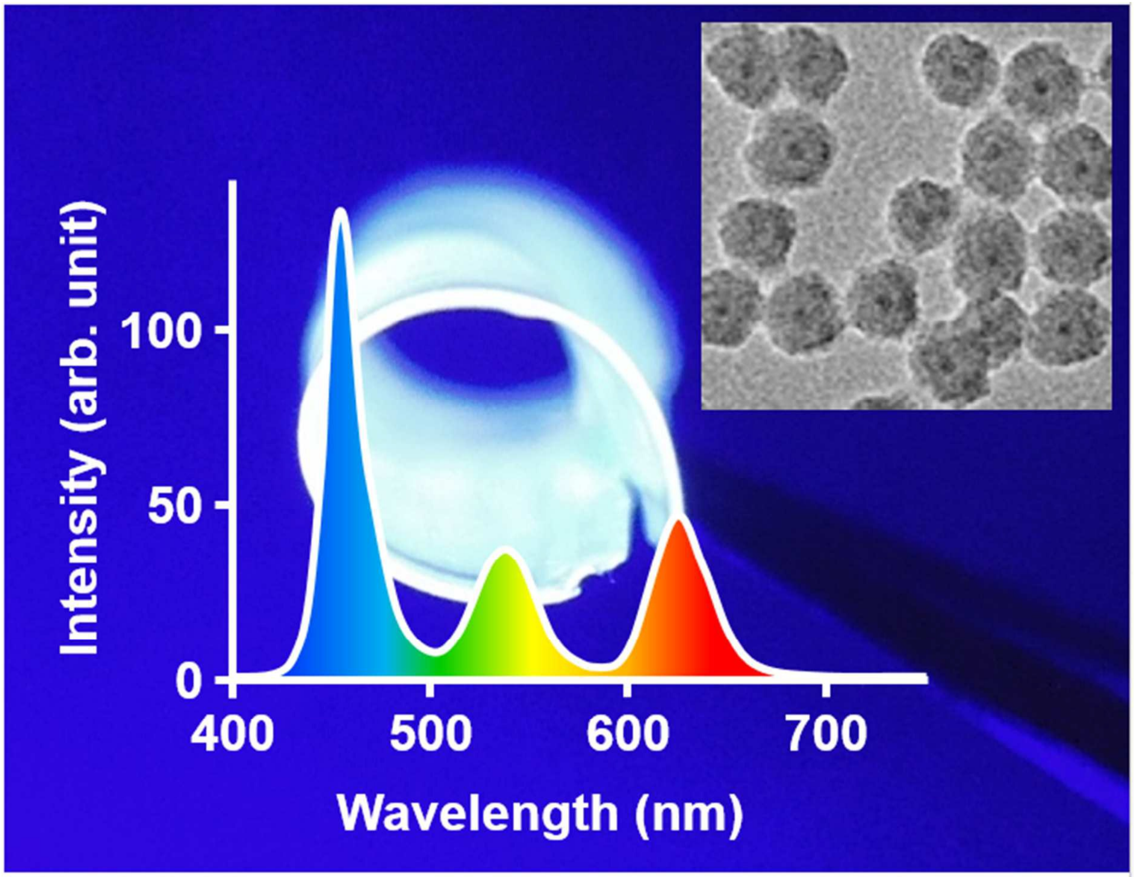

The dimethylamine (DMA) catalyst played a major role in maintaining the original luminescence of the quantum dots (QDs) when forming the silica shells during the sol-gel condensation. The silica shell was a good barrier against oxidation, and thus, the SiO2 coated QD (QD@SiO_2) with green or red fluorescent exhibited high photo- and thermal- stability and retained their initial photoluminescence (PL) intensity. A white light-emitting diode (WLED) was fabricated with a mixture of green and red light-emitting QDs@SiO_2 in flexible polymer nanocomposite film. QD@SiO2 particles were exhibited excellent WLED performance owing to the high stability.